SHIMADZU
Excellence in Science

Technical Report

Multiple Analytical Techniques For Carotenoid Analysis In Capsicum Cultivars

Francesco Cacciola[1], Katia Arena[1], Mariosimone Zoccali[1], Luigi Mondello[1]

Abstract:

Carotenoids and their derivatives are versatile isoprenoids based on a C40 tetraterpenoid skeleton and play a vital role in plants and animals, but, due to their high variability in the chemical structures, isomerization, poor stability and lack of commercially available standards, their identification in real samples is a challenging task. For this reason, different extraction and separation techniques have been tested, in particular: an online coupling between supercritical fluid extraction (SFE) and supercritical fluid chromatography (SFC), a reversed-phase separation in high-performance liquid chromatography by using two serially coupled C30 columns and a comprehensive normal-phase × reversed-phase liquid chromatography (NP-LC×RP-LC) system. As far as detection is concerned, PDA and MS detection was used in all the systems, with the exception of the SFE-SFC analysis where only MS was used.

Keywords: Food、Natural Pigments、carotenoids、HPLC、SFC、LC x LC

1. ARTICLE CONTENT

Carotenoids are natural pigments synthesized by plants and some microorganisms. Humans and animals are not able to synthesize carotenoids de novo and they need to acquire them through their diet. The most significant aspect of carotenoids in our diet is the antioxidant and provitamin A activity, and also the color that they impart to our food [1]. Carotenoids are based on a C40 tetraterpenoid skeleton which can undergo a high diversity of modifications, such as cyclization in one or both ends, hydrogenation, dehydrogenation, addition of lateral groups, among others, resulting in more than 600 different carotenoids identified in nature [2]. Usually, these compounds are divided into two groups: hydrocarbons, composed of only carbon and hydrogen such as lycopene and β-carotene (commonly known as carotenes) and oxygenated compounds (generally named xanthophylls), which are oxygenated and may contain epoxy, carbonyl, hydroxy, methoxy or carboxylic acid functional groups.

To further increase the natural variability of these compounds, it has to be considered that carotenoids can be present in nature as free carotenoids or in a more stable form esterified with fatty acids, in the case of the oxygenated compounds. To simplify in some extent their analysis, a saponification procedure has been traditionally employed to release all the carotenoid esters and to analyze all these compounds in their free form. Although this saponification step acts also as a clean-up procedure, some drawbacks are found, mainly related to the formation of artefacts as well as to the production of carotenoid degradation.

Moreover, as a result of the saponification step, information on the native carotenoids composition of the studied samples is therefore lost. Thus a better approach to carotenoid content is through classifying plant materials depending on a free or esterified xanthophylls profile. In fact the carotenoid esters could be used as a marker of authenticity of food products and could be useful as a ripeness degree index; moreover, esters may enhance food products oxidative stability and may improve carotenoids bioavailability. Although esterification does not change the chromophore properties of the carotenoid molecules, it does modify the immediate molecular environment.

As a consequence, chemical activities may be altered depending on the kind of fatty acid bound to the xanthophylls [3]. Capsicum are one of the oldest and most popular vegetables and spices in the world. Their species uniquely have capsanthin-capsorubin synthase that synthesizes two red pigments, capsanthin and capsorubin. Moreover, carotenoids esterification greatly increases during the fruits ripening process. Therefore, in this contribution, the carotenoid composition in different Capsicum species was elucidated by developing different analytical systems e.g. an online SFE-SFC system coupled with a QqQ MS detector, which compared to offline approaches, improves run-to-run precision, enables the setting of batch-type applications, and reduces the risks of sample contamination; an LC method which allowed the direct identification of the carotenoids in the samples, based on the use of serially connected C30 columns coupled with PDA and APCI-MS detectors and a novel NP-LC×RP-LC system, consisting of a micro-bore (1.0 mm i.d.) cyano column for the first dimension (^{1}D) separation, interfaced to a second dimension (^{2}D) 2.7 µm C18 column packed with fused-core particles (30×4.6 mm) and coupled with PDA and MS detectors. Moreover, in the latter case, operating in UHPLC conditions and made by two columns of the same stationary phase coupled serially in the ^{2}D, was tested.

2. MATERIALS AND METHODS

SFE-SFC

Samples and sample preparation

In the on-line supercritical fluid extraction supercritical fluid chromatography (SFE–SFC) approach, the habanero sample (1 g) was grinded by using the ultra-turrax and homogenized with an absorbent powder (1 g) and placed in the extraction vessel in the SFE unit. A 0.2 mL extraction vessel was used, loaded with 100 mg of sample/adsorbent. Supercritical CO_2 was then introduced into the vessel, where extraction conditions were optimized with respect to pressure and temperature. After extraction in the SFE unit, the sample-containing CO_2 was directed in the SFC flow line for performing the following chromatographic analysis.

SFE-SFC instrumentation

SFE-SFC-MS analyses were performed on a Shimadzu Nexera-UC system, consisting of a CBM-20A controller, an SFE-30A module for supercritical fluid extraction, two LC-20AD$_{XR}$ dual-plunger parallel-flow pumps, an LC-30AD$_{SF}$ CO_2 pump, two SFC-30A back pressure regulator, a DGU degasser, a CTO-20AC column oven, a SIL-30AC autosampler, an LCMS-8050 triple quad mass spectrometer equipped with an APCI source. The entire system was controlled by the LabSolutions ver. 5.8.

Chromatographic method

SFE: Solvent: (A) CO_2; (B) methanol; Gradient: 50% B; 1.1 min 0% B; Flow rate: 0-1 min 2 mL/min; 1-4 min 3 mL/min; 4-20 min 2mL/min; Extraction mode: 0-3 min static mode, 3-4 dynamic mode; Extraction vessel temperature: 40, 50, 50, 60, 70 and 80°C; **SFC**: Analytical column: A core-Shell C30 Column, 150×4.6 mm, 2.7 µm d.p.; Mobile phase: (A) CO_2; (B) methanol; (make-up) methanol; Gradient: 0-2 min, 0% B; 2-10 min 40% B; 10-13 min 40% B; Flow rate: 2 mL/min; Column oven: 35°C; Back Pressure regulator A: 150 bar; MS Acquisition mode: SCAN (+)/(-); SIM (+)/(-); MRM (+);

RP-HPLC

Samples and sample preparation

Fresh samples of green, yellow and red sweet bell peppers were supplied by a local producer.

Carotenoid standards, namely, β-carotene, lutein, β-cryptoxanthin, zeaxanthin, capsanthin and lutein-di-palmitate (C16:0, C16:0) were purchased from Extrasynthese (Genay, France). All the carotenoid standards were stored protected from light at -18°C. All the solvents used, namely, methanol, methyl tert-butyl ether (MTBE) and water, were HPLC grade and purchased from Sigma-Aldrich (Milan, Italy). BHT (butylatedhydroxy toluene) and potassium hydroxide were obtained from Sigma-Aldrich (Milan, Italy).

Extraction

The sweet bell peppers samples (200 g) were homogenized, and the carotenoids were extracted four times with methanol/ethyl acetate/petroleum ether (1:1:1, v/v/v). The upper phase was kept and ca. 2 mg of BHT were added prior evaporation under vacuum until dryness. The dry residue was then resuspended in a given volume of MTBE/methanol (1:1) and stored protected from light at -18°C until use.

RP-HPLC analysis

To carry out the analyses a Shimadzu HPLC instrument (Kyoto, Japan) equipped with a CBM-20A controller, two LC-20AD dual-plunger parallel-flow pumps, a DGU-20A$_{5R}$ degasser, a CTO-20AC column oven, a SIL-30AC autosampler, an SPD-M20A photo diode array detector, and an LCMS-2020 mass spectrometer, through an atmospheric pressure chemical ionization (APCI) source operated in both positive and negative ionization mode (Shimadzu, Kyoto, Japan). Data acquisition was performed by Shimadzu LabSolutions software ver. 5.91.

The APCI parameters were set as follows: mass spectral range 100-1200 m/z; interval: 0.5 sec; nebulizing gas (N2) flow: 3 L/min; interface temperature: 400 °C; Heat block: 400 °C, DL temperature: 250 °C; DL voltage -34 V; probe voltage 4.5 kV; Qarray voltage: 1.0 V, RF voltage: 90 V; detection gain 1.0 kV.

The C30 columns employed consisted of two C30 analytical columns with 5 µm C30 reversed-phase material (250 × 4.6 mm I.D.), including a pre-column (YMC 30; S-5 µm, 10 × 4.0 mm I.D.).

The HPLC solvent systems were (A) methanol/MTBE/water (83:15:2, v/v/v) and (B) methanol/MTBE/water (8:90:2, v/v/v) used following a linear gradients depending on the use of one or two serial coupled columns. Gradient for the separation with 1 x C30 column: 0-20 min, 0% B; 20-160 min 100% B; then reconditioning. Gradient for the separation with 2 x C30 columns: gradient times were doubled keeping unchanged the B%. The flow rate employed was 1 mL/min and the chromatograms were recorded at 450 nm and the UV-Vis spectra were recorded in the range from 250 to 600 nm (sampling rate: 12.5 Hz; time constant: 0.64 s). The column oven temperature was 40 °C.

NP-LC×RP-LC and NP-LC×UHPRP-LC

Samples and chemicals

Methanol, ethyl acetate, petroleum ether and tert-butyl methyl ether, all reagent grade, for sample preparation were supplied by Sigma-Aldrich (Milan, Italy). LC-MS grade solvents for LC×LC and LC×UHPLC analyses, water (H_2O), isopropanol (IPA), and acetonitrile (ACN) were purchased from Sigma-Aldrich (Milan, Italy). LC grade hexane (Hex), butylacetate and acetone were obtained from VWR (Milan, Italy).

The red chili pepper sample (*Capsicum annuum L.*) was purchased in a local market. For the extraction of intact carotenoids, 200 g of red chili pepper homogenate were treated with three consecutive 300-mL aliquots of a methanol/ethyl acetate/petroleum ether (1:1:1, v/v/v) mixture. Combined extracts were then dissolved in 4 mL of methanol/tert-butyl methyl ether (1:1, v/v) and afterward subjected to filtration through a 0.45 mm Acrodisc nylon membrane filter (Pall Life Sciences, Ann Arbor, MI, USA).

NP-LC×RP-LC and NP-LC×UHPRP-LC instrumentation

LC×UHPLC analyses were performed on a Shimadzu Nexera-e system (Shimadzu, Kyoto, Japan), consisting of a CBM-20A controller, four LC-30AD dual-plunger parallel-flow pumps, a DGU-20$_{A5}$ degasser, an SPD-M20A photo diode array detector, a CTO-20A and a CTO-30A column ovens, a SIL-30A autosampler. The two dimensions were connected by means of two high speed/high pressure two-position, six-ports switching valves with micro-electric actuator (model FCV-32 AH, 1.034 bar; Shimadzu,

Kyoto, Japan), placed inside the column oven and equipped with two 0.254 mm I.D. stainless steel sample loops of identical volume. Both dimensions and the switching valve were controlled by the LCMSsolution® software (Version 3.50.346, Shimadzu). The LC×LC data were visualized and elaborated into two and three dimensions using Chromsquare ver. 1.5 software (Chromaleont, Messina, Italy). The LC×LC system was coupled to an LCMS-IT-TOF mass spectrometer through an APCI source (Shimadzu, Kyoto, Japan).

Columns

One core shell cyano column, 250x1.0 mm, 5 mm d.p. was used as ^{1}D. In the LC×LC system, one core shell C18 column, 30x4.6 mm, 2.7 mm d.p. was used as ^{2}D, while in the LC×UHPLC system two columns of the same type were serially connected by means of 0.1 mm ID stainless steel tubing.

NP-LC×RP-LC conditions

Set-up #1. ^{1}D mobile phase: (A) *n*-hexane; (B) *n*-hexane/butyl-acetate/acetone (80:15:5, v/v/v). Gradient: 0-5 min, 100% A; 5-65 min, to 0% A; hold for 45 min. Mobile phase flow rate: 10 mL/min. Column oven: 30 °C. Injection volume: 2 µL.
^{2}D mobile phase: (A) water/ACN (10:90, v/v); (B) IPA. Gradient: 0.01 min, 30% B; 0.12 min, to 50% B; hold for 0.08 min; 0.40 min, to 80% B; hold for 0.30 min; 0.71 min, to 30% B; hold for 0.04 min. Mobile phase flow rate: 4 mL/min. Column oven: 65 °C. Modulation time of the switching valves: 0.75 min.
PDA detection: 250-550 nm (sampling rate, 12.5 Hz; time constant, 0.08 s).
LCMS-IT-TOF detection: one milliliter flow from the second dimension of the LC×LC or LC×UHPLC system was directed to the mass spectrometer, through APCI interface operated in positive and negative ionization mode. Detector voltage, 1.50 kV; interface temperature: 400 °C; CDL temperature, 250°C; block heater temperature, 250 °C; nebulizing gas flow (N_2), 2.5 L/min; ion accumulation time, 30 ms; full scan range, 200-1200 m/z; event time, 300 ms; repeat, 3; ASC, 70%.

NP-LC×UHPRP-LC conditions

Set-up #2. Modulation time of the switching valves: 1.50 min. Gradient: 0.01 min, 30% B; 0.25 min, to 50% B; hold for 0.15 min; 0.80 min, to 80% B; hold for 0.60 min; 1.41 min, to 30% B; hold for 0.09 min. Mobile phase flow rate: 4 mL/min. Column oven: 65 °C.
Set-up #3. Modulation time of the switching valves: 1.00 min. Gradient: 0.01 min, 30% B; 0.17 min, to 50% B; hold for 0.10 min; 0.54 min, to 80% B; hold for 0.39 min; 0.94 min, to 30% B; hold for 0.06 min. Mobile phase flow rate: 4 mL/min. Column oven: 65 °C.

3. RESULTS AND DISCUSSION

SFE-SFC

An SFE-SFC-APCI-QqQ/MS method for the direct identification of the native carotenoid composition in habanero red (*Capsicum* chinense) sample was developed. Compounds were identified by comparison with the available standards, by using the elution

Table 1. MS APCI (+) and APCI (-) information for the identification of the carotenoids and chlorophylls analysed in this work.

ID	Identification	MS data APCI (+) e (-)
1	Luteoxanthin	601, 583 (+) ; 600 (-)
2	Antheraxanthin	585, 567 (+) ; 584 (-)
3	cis-Capsanthin	585, 567(+) ; 584 (-)
4	(13Z)-cis-Cryptocapsin	569 (+) ; 568 (-)
5	Chlorophyll b	907 (+) ; 906 (-)
6	Lutein	551 (+) ; 568 (-)
7	Capsanthin	585, 567, 479 (+) ; 584, 478 (-)
8	Zeaxanthin	569 (+) ; 568 (-)
9	Chlorophyll a	893 (+) ; 892 (-)
10	(13Z) -cis-β-Cryptoxanthin	553 (+) ; 552 (-)
11	Cryptocapsin	569 (+) ; 568 (-)
12	Phytoene	545 (+) ; 544 (-)
13	Cryptoxantin-5,6-epoxide	569 (+) ; 568 (-)
14	α-Cryptoxanthin	553 (+) ; 552 (-)
15	(9Z)-cis-α-Carotene	537 (+) ; 536 (-)
16	β-Cryptoxanthin	553 (+) ; 552 (-)
17	Phytofluene	543 (+) ; 542 (-)
18	β-Carotene-5,6-epoxide	553 (+) ; 552 (-)
19	β-Carotene-5,8-epoxide	553 (+) ; 552 (-)
20	(13Z)-cis-β-Carotene	537 (+) ; 536 (-)
21	α-Carotene	537 (+) ; 536 (-)
22	cis-Capsanthin-C12:0	767, 567 (+) ; 766 (-)
23	cis-Capsanthin-C12:0	767, 567 (+) ; 766 (-)
24	Antheraxanthin-C14:0	795, 567 (+) ; 794 (-)
25	β-Carotene	537 (+) ; 536 (-)
26	Capsanthin-5,6-epoxy-C14:0	811, 583 (+) ; 810 (-)

ID	Identification	MS data APCI (+) e (-)
27	Pheophytin a	872 (+) ; 871 (-)
28	cis-Capsanthin-C14:0	795, 567 (+) ; 794 (-)
29	Lutein-C14:0	779, 551 (+) ; 778 (-)
30	Capsanthin-C12:0	767, 567 (+) ; 766 (-)
31	Zeaxanthin-C12:0	751, 551 (+) ; 750 (-)
32	Capsanthin-C14:0	795, 567 (+) ; 794 (-)
33	Zeaxanthin-C14:0	779, 551 (+) ; 778 (-)
34	Capsanthin-C16:0	823, 567 (+) ;822 (-)
35	Zeaxanthin-C16:0	807, 551 (+) ; 806 (-)
36	β-Cryptoxanthin-C12:0	735, 535 (+) ; 734 (-)
37	Cryptocapsin-C14:0	779, 551 (+) ;778 (-)
38	β-Cryptoxanthin-C14:0	763, 535 (+) ;762 (-)
39	Cryptocapsin-C16:0	807, 551 (+);806 (-)
40	β-Cryptoxanthin-C16:0	791, 535 (+); 790 (-)
41	Capsanthin-C12:0, C14:0	977, 777, 749, 549 , 976 (-)
42	Zeaxanthin-C12:0, C12:0	933, 733, 533 , 932 (-)
43	Capsorubin-C14:0, C14:0	1021, 793, 565 , 1020 (-)
44	Zeaxanthin-C12:0, C14:0	961, 733, 533 (+) ; 960, 760 (-)
45	Capsanthin-C14:0, C14:0	1005, 777, 549 (+) ; 1004 (-)
46	Capsorubin-C14:0, C16:0	1049, 821, 793, 565 (+) ; 1048 (-)
47	Capsanthin-C12:0, C16:0	1005, 805, 749, 549 (+) ; 1004 (-)
48	Zeaxanthin-C14:0, C14:0	989, 761, 533 (+) ; 988, 760 (-)
49	Capsanthin-C14:0, C16:0	1033, 805, 777, 549 (+) ; 1032 (-)
50	Zeaxanthin-C14:0, C16:0	1017, 789, 761, 533 (+) ; 1016 (-)
51	Capsanthin-C16:0, C16:0	1061, 805, 549 (+) ; 1060 (-)
52	Zeaxanthin-C16:0, C16:0	1045, 789, 533 (+); 1044, 788 (-)

order, and by their MS spectra recorded in both positive and negative APCI ionization modes, the possibility of rapid switchover between negative and positive ionisation mode in the APCI probe allowed us to collect more qualitative information about a sample in a single run, with quasi-molecular ion species dominating the MS spectrum in one case (negative mode), or abundant fragmentation in the other (positive mode).

Moreover three components were pinpointed by using the multiple reaction monitoring (MRM), namely Capsanthin, Lutein, and Zeaxanthin. The SFE has been optimized using different temperatures, starting from 40°C up to 80°C using an increase of 10 degrees. Multiple extractions, until depletion, were performed on the same sample, in order to evaluate the extraction yield. For all the compounds considered, in the fourth extraction only some traces were eventually present. Totally 21 analytes were extracted and identified, considering the average of the first extraction among all the compounds, it can be noted an increasing trend in the extraction yield, by increasing temperature: 40° C average 41.8% (min. value 35.9%, max value 51.2%), 50 ° C average 46.4% (min. value 38.0%, max value 55.0%), 60 ° C average 46.7% (min. value 39.5%, max value 53.4%), 70 ° C average 47.1% (min. value 38.3%, max value 54.8%), and 80° C average 48.6% (min. value 37.4%, max value 65.4%).

In Table 1 are reported the MS [APCI (+) and APCI (-)] ions used for the identification of the carotenoids and chlorophylls. In Figure 1 is reported an expansion of the chromatogram (SIM) with peak identifications of the free carotenoids.

As can be observe six different components were identified, respectively: α Carotene, β Carotene, Capsanthin, Lutein, Zeaxanthin, and Chlorophyll b. α and β Carotene appear to be co-eluted, due to their high amount. In Figure 2 is reported the expansion (SIM) of mono-ester carotenoids area of the chromatogram. Ten different components were identified: Antheraxanthin-C12:0 and C14:0, Capsanthin-C12:0, C14:0, and C16:0, cis-Capsanthin-C12:0 and C14:0, Lutein-C16, Zeaxanthin-C16:0, and β-Cryptocapsin. In Figure 3 is reported the expansion (SIM) of di-ester carotenoids area of the chromatogram. Four components were identified belonging to the Capsanthin family: Capsanthin-C12:0,C14:0; C12:0,C16:0; C14:0,C16:0; and C16:0,C16:0. Finally, to evaluate the performance of the MS system, the MRM acquisition mode was used simultaneously. In Figure 4 is reported the expansion of the same area reported in Figure 1, showing the MRM acquisition for Capsanthin (585<109 CE 40 eV and 585<145 CE 20 eV), Lutein (569<119 CE 40 eV and 569<133 CE 20 eV), and Zeaxanthin (569<119 CE 40 eV and 569<133 CE 20eV).

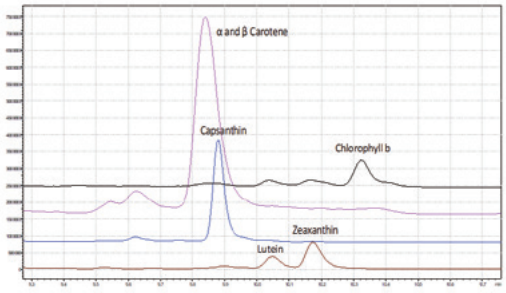

Figure 1. Expansion of the free carotenoids zone acquired in SIM mode of a red habanero sample.

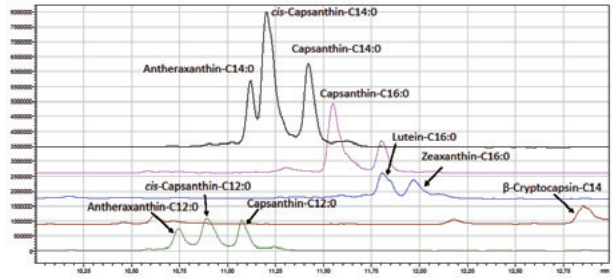

Figure 2. Expansion of the carotenoids mono-ester zone acquired in SIM mode of a red habanero sample.

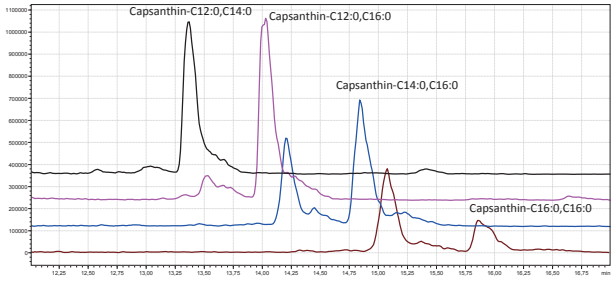

Figure 3. Expansion of the carotenoids di-ester zone acquired in SIM mode of a red habanero sample.

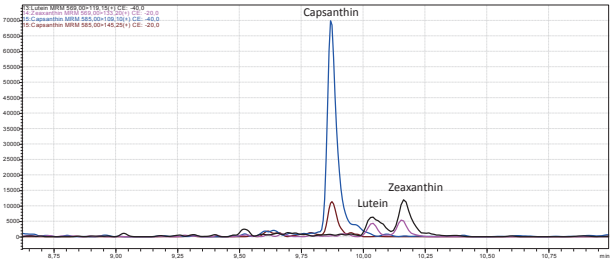

Figure 4. Expansion of the same chromatogram zone reported in Figure 1 but acquired by MRM.

RP-HPLC

High performance liquid chromatography is considered as the selected analytical tool for a huge number of application, including the carotenoid analysis. However, due to the great complexity of some natural samples containing this kind of compounds, conventional LC could not have enough separation power. In this work, serial connection of two columns is proposed as an alternative to conventional LC. The applicability of connecting two C30 columns to significantly increase the separation power, resolution and peak capacity for the analysis of carotenoids in sweet bell peppers has been demonstrated. Moreover, here we report the first investigation of the native carotenoid profile in sweet bell peppers at three different ripening stages: green, yellow and red (Figures 5, 6 and 7).

As shown in Figure 7B, 56 different carotenoids have been detected in red sweet bell peppers, including many esters, (for peaks identification see Table 2). No carotenoids esters were detected in yellow or green sweet bell peppers. The identification of these compounds was carried out combining the information provided by the two detectors employed (i.e., PDA and APCI-MS detectors) and the commercial standards available. As can be observed in figure 7, the order of elution of the different compound its highly dependent of the polarity and hydrophobicity of the molecules. Therefore, free xanthophylls will elute before mono-esterified one, and the di-esterified xanthophylls will have longer retention times. By considering the different fragmentations in the APCI-MS producing different regioisomers, various xanthophylls di-esters were detected in red bell peppers.

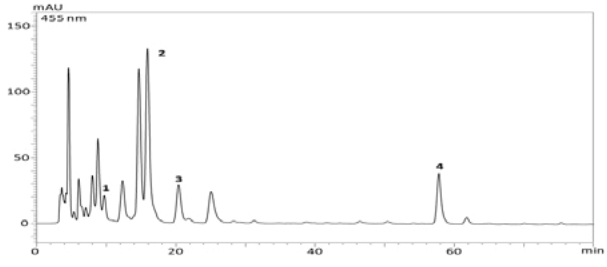

Figure 5. Chromatograms (455 nm) of Sweet Bell Green Peppers using one C30 column.
Peak identification: 1 Luteoxanthin; 2 Lutein; 3 Zeaxanthin; 4 β-carotene.

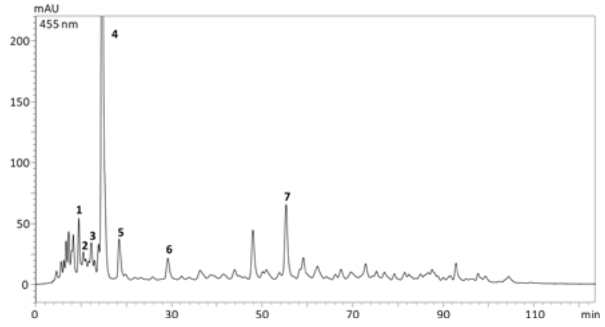

Figure 6. Chromatograms (455 nm) of Sweet Bell Yellow Peppers using one C30 column.
Peak identification: 1 Luteoxanthin; 2 Auroxanthin; 3 Antheraxanthin; 4 Lutein; 5 Zeaxanthin; 6 β-cryptoxanthin; 7 β-carotene.

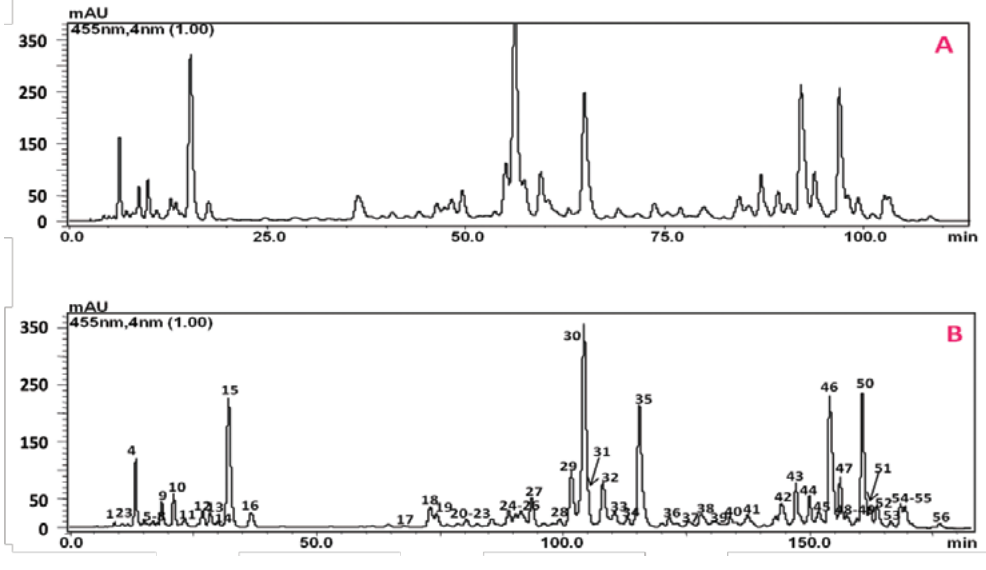

Figure 7. Chromatograms (455 nm) of Sweet Bell Red Peppers using one C30 column (A), and two C30 columns (B). For peaks identification see Table 2.

Table 2. UV-Vis, MS information and identification of the different carotenoids separated in Sweet Bell Red Pepper using two serially connected C30 columns.

N°	Peak identification	λ max (nm)	[M + H]+
1	Neoxanthin	416,440,469	601,583
2	n.i.	419,446,467	601,583
3	β-apo-10-carotenal	436	376,361
4	Violaxanthin	418,441,470	601,583
5	Luteoxanthin	400,422,448	601,583
6	n.i.	418,440,467	613,595
7	n.i.	400,424,448	601,583
8	n.i.	400,423,448	615,597
9	Capsanthin-5,6-epoxide	469,486	601,583,565
10	Anteraxanthin	424s,445,474	585,567
11	n.i.	357,448,469	585,567
12	Mutatoxanthin A	406,429,451	585,567,549
13	n.i.	457s,479,507	601,583,567,491
14	Mutatoxanthin B	406,429,452	585,567,549
15	Capsanthin	474	585,567,479
16	Zeaxanthin	427,451,477	569,551,476
17	Phytofluene	332,348,367	543
18	β-cryptoxanthin	426,451,477	553,535
19	Anteraxanthin-laureate (C12:0)	422,447,474	767,749,567
20	n.i.	400,424,448	875,597
21	n.i.	424,443,469	875,597,565
22	n.i.	451,467	823,583
23	n.i.	425s,447,467	877,823,597
24	n.i.	466	879,599,583
25	n.i.	400,424,448	879,793,597
26	Anteraxanthin-myristate (C14:0)	424,446,474	795,777,567
27	n.i.	425,446,474	876,777
28	Mutatoxanthin-laureate (C12:0)	408,425,452	767,749,567
29	Capsorubin-myristate (C14:0)	479	811,583,565
30	β-carotene	452,478	537
31	Capsanthin-laureate (C12:0)	474	767,567,549
32	Anteraxanthin-myristate (C14:0)	425,447,474	795,777,567
33	n.i.	424s,448,471	853,795,567
34	Mutatoxanthin-myristate (C14:0)	406,429,452	795,777,567
35	Capsanthin-myristate (C14:0)	474	795,777,567
36	n.i.	460	795,567,549
37	n.i.	426,451,474	879,684,533
38	n.i.	424,443,469	961,821,547
39	n.i.	466,472	823,567,549
40	β-cryptoxanthin-laureate (C12:0)	426,451,477	735,535
41	n.i.	469	765,549
42	β-cryptoxanthin-miristate (C14:0)	425,452,479	765,535
43	Capsanthin-di-laureate (C12:0,C12:0)	473	949,749,549
44	Capsorubin-laureate-myristate (C12:0,C14:0)	479	993,793,765,565
45	n.i.	428,451,470	1,021,793,565
46	Capsanthin-laureate-myristate (C12:0,C14:0)	474	977,777,749,549
47	Capsorubin-di-myristate (C14:0,C14:0)	481	1,021,793,565
48	Mutatoxanthin-laureate-myristate (C12:0,C14:0)	406,429,454	977,793,765,565
49	Zeaxanthin-laureate-myristate (C12:0,C14:0)	425,451,478	961,761,733,533
50	Capsanthin-di-myristate (C14:0,C14:0)	474	1,005,777,549
51	n.i.	469	1,005,777,749,549
52	Capsorubin-myristate-palmitate (C14:0-C16:0)	479	1,049,821,793,565
53	Zeaxanthin-di-myristate (C14:0,C14:0)	427,452,477	989,761,533
54	Capsanthin-myristate-palmitate (C14:0,C16:0)	474	1,033,805,777,549
55	n.i.	469	805,777,549
56	n.i.	469	805,713,549,551

Table 3. Values of Peak capacity (nc) and resolution (Rs) between selected peaks for the analysis of Sweet Bell Red Peppers using two different set ups.

Set Up	nc	Rs(12-13)	Rs(29-30)	Rs(32-33)
1×C30	73.0	0.23	0.66	0.30
2×C30	95.4	0.85	1.28	0.85

As can be seen in Table 3, by using two serially coupled C30 columns a peak capacity of 95.4 was obtained, compared to 73 achieved using a single column. Moreover, the resolution values of some critical pairs (12-13, 29-30 and 32-33) were significantly improved by the coupling of the two C30 columns.

Interestingly, free carotenoids, mono-esters and di-esters were quantitatively equally represented (around 33% for each different class) in red sweet bell pepper, and the ratio di-esters/mono-esters was around 1, which could be considered a typicality parameter of red peppers. β-carotene (6%), lutein (20-30%) and zeaxanthin (2-5%) were the most abundant carotenoids present in yellow and green sweet bell peppers, whereas violaxanthin (2.2%) capsanthin (8.1%) and β-carotene (12.6%) characterised the free carotenoids fraction of sweet red bell peppers. Myristic acid (C14:0) was the most abundant fatty acid present as mono-ester with capsanthin (8.4%), capsorubin (3.1%) and antheraxanthin (2.7%) in red bell peppers.

Lauric and myristic acids were mainly present in the di-esters of capsanthin and capsorubin, in red bell peppers. In particular, the most abundant di-esters in red bell peppers were capsanthin-C12:0, C14:0 (8.9%), capsanthin-C14:0, C14:0 (7.1%) and capsorubin-C14:0, C14:0 (3.3%). No carotenoid esters were detected in both green and yellow sweet bell peppers. Interestingly, Minguez-Mosquera [4] reported that in the yellow spicy *Capsicum annuum* of the cultivar Bola, already 50% of the carotenoids were esterified, and that at the fully ripened red stage the percentages of the free carotenoid pigments and the partially and totally esterified forms of these were 21.3%, 35.6%, and 43.1% respectively, therefore different from the percentages reported in this work for the red sweet bell peppers, where the three fractions were equally represented. The increase of the xanthophylls esterification during ripening reported in this work, is in agreement with the report by Hornero-Mendez [5] for various cultivars of spiced *Capsicum annuum* cultivars. This process and inherent to the degeneration of chloroplast and formation of chromoplast. Such phenomenon might be the result of a hydrophobicity requirements on the part of the carotenoid, so that with all its hydroxyl groups esterified it will be included more readily in the lipid matrix of chromoplast membranes and organelles (plastoglobules) [5].

Schweiggert et al. [6] reported that capsanthin and β-carotene were the main free carotenoids in spiced red peppers, in agreement with the results reported in this work for sweet red bell peppers, and they reported also a similar esters profile for spicy red peppers pods, although the sweet bell red peppers analysed in this work showed an higher degree of esterification with capsanthin rather than with capsorubin.

NP-LC×RP-LC and NP-LC×UHPRP-LC

NP-LC×RP-LC conditions

An LC×LC platform was first implemented, consisting of normal-phase chromatography and reversed-phase chromatography in the first and the second dimension, respectively. NP-LC×RP-LC represents one of the most orthogonal approaches in two-dimensional liquid chromatography, capable to afford very high resolution power due to independent separation mechanisms operating on the individual stationary phases. The NP-LC×RP-LC coupling is not easy and straightforward to achieve, due to the incompatibility of the solvents that are used in the two dimensions, and possible problems of peak focusing at the head of the 2D [7-9]. Such practical constraints were successfully circumvented in approaches previously developed by our research group, based on the combination of a micro-bore column in the first dimension and either a monolithic or a fused-core column in the 2D [7-10]. In this work, 1D and 2D separations were optimized independently, then combined and tuned together. In the first dimension, a 250x1.0 mm, 5 mm-d.p. cyano column was operated under linear gradient conditions, starting from 100% *n*-hexane (A, 0-5 min) and going to 100% (B) *n*-hexane/butyl-acetate/acetone (80:15:5, v/v/v) in 60 min (hold for 45 min). A mobile phase flow rate of 10 mL/min gave the best results, in terms of peak overlap and resolution, for carotenoid separation into classes of increasing polarity (as discussed later on).

Subsequently, applications were run on a fully automated LC×LC system, configured around two electronically activated two-position, six-ports switching valves for within-loop automated fraction collection/re-injection, equipped with two storage loops of identical volume. In the comprehensive set-up, the whole effluent from the 1D micro-bore column was transferred on-line to the 2D column, consisting of a 3 cm length, 4.6 mm i.d. of a C18 fused-core column (2.7 mm d.p.). The 1D effluent was therefore fractionated every 0.75 min, with a modulation time (cycle time) of the switching valves corresponding to the 2D analysis time. The choice of switching valves modulation time and gradient profile was made to meet the following stringent requirements: each fraction injected onto the 2D column must be completely eluted before the following transfer occurs; the 2D analysis time has to be kept as short as possible, not to impair the separation achieved in the 1D (in this respect, a large number of cuts is highly beneficial). For all these reasons, the 2D separation must be fast and on-column focusing must be achieved; these requirements were fulfilled with the employment of a very high flow rate (4 mL/min) and a gradient program starting with high concentration (70%) of the weaker solvent.

A fast ramp up to 80% of the stronger solvent (IPA) was run at the end of the gradient, to ensure the elution of all the components within a fast analysis time of 0.75 min, including reconditioning time of 0.04 min. Repetitive injections of the sample under such conditions afforded perfectly super-imposable elution profiles (data not shown), thus ensuring sufficient column re-equilibration time after the gradient. In Figure 8 A-B, a schematic of the LC×LC system is depicted, showing the routes for each second dimension separation, to which PDA and LCMS-IT-TOF detectors were serially connected, for identification of the separated compounds. In this regard, the use of RP-LC as 2D of a two-dimensional system also provides excellent compatibility with MS detection, as already demonstrated by a number of research works; especially using fused-core stationary phase either to attain enhanced resolving power, or to perform fast repetitive analyses under gradient conditions [11-14].

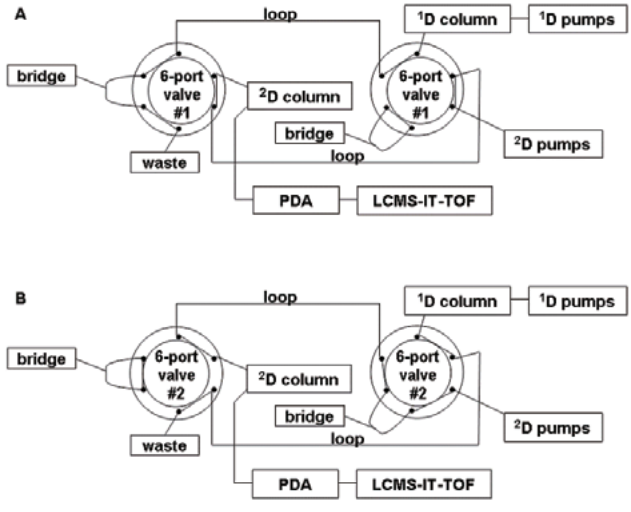

Figure 8 A-B. Schematic of the LC×LC system employed in this work, showing the routes for each second dimension separation, corresponding to different positions of the two six-port, two-position switching valves.

Results obtained from the NP-LC×RP-LC analysis of free carotenoids and carotenoid esters in the red chili pepper extract are shown in the contour plot of Figure 9, extracted at a 450 nm wavelength, under an experimental backpressure of 440 bar, which is the maximum allowed on a conventional HPLC instrument (set-up #1).

Chromatography on the cyano stationary phase allowed a good separation of the carotenoids in groups of different polarity in the first dimension, as can be seen from the ellipses in Figure 9, with retention times increasing in the order: hydrocarbons < mono-ol-esters < di-ol-di-esters < di-ol-mono-epoxide-di-esters < di-ol-mono-keto-di-esters < free-mono-ols < di-ol-mono-epoxide-mono-esters < di-ol-di-keto-di-esters < di-ol-di-keto-mono-esters < poly-oxygenated-free-xanthophylls.

On the other hand, the C18 column allowed the separation of carotenoids within each class, according to their increasing hydrophobicity and decreasing polarity (for components of the same class, the elution order increases with the number of carbon atoms of the fatty acid chain).

By optimizing the elution parameters (as a compromise between the chromatographic separation, modulation time, maximum column operating temperature, and highest flow rate allowed by the system backpressure limit), a satisfactory separation of the sample carotenoids was obtained, with ten different classes distributed along characteristic chemical patterns in the 2D retention plane. However, some co-elutions were observed, especially in the free-xanthophyll and, to a lesser extent, in the di-ol-mono-keto-mono-ester classes.

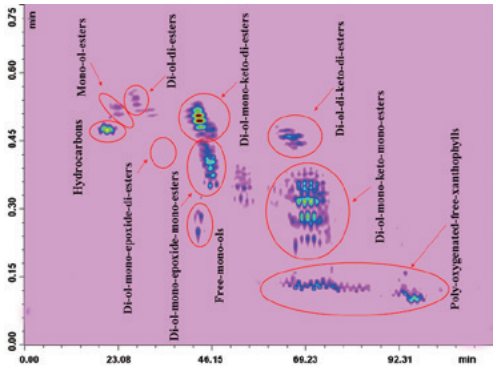

Figure 9. Contour plot of the NP-LC×RP-LC analysis of free carotenoids and carotenoid esters present in a red chili pepper extract with a modulation time of 0.75 min (PDA chromatogram extracted at 450 nm).

65 °C. Results obtained from the NP-LC×RP-UHPLC analysis of free carotenoids and carotenoid esters in the red chili pepper extract are shown in the contour plot of Figure 10, extracted at a 450 nm wavelength. The improvement in separation power obtained under such conditions is clear from a visual inspection of the 2D plot, especially for the free-xanthophyll and the di-ol-mono-keto-mono-ester classes. Identification of the separated compounds was achieved by means of both PDA and LCMS-IT-TOF detection (through APCI ionization). The latter represents a powerful analysis tool for unknown molecules; especially in the case of carotenoids, operation of the interface under both positive and negative mode offers the double advantage of improved sensitivity and/or identification power. MS spectra obtained under negative ionisation mode are in fact dominated by the presence of very intense pseudomolecule ions [M].-, which make identification/quantitation of low-abundant components easier; on the other hand, abundant fragmentation is, generally, observed under positive APCI ionization, especially for carotenoid esters, whose fragment ions can help in structure elucidation through dedicated software/database. It must be also stressed that a better front-end LC separation is highly beneficial prior to MS analysis, since clearer spectra are obtained. This represents a stringent requirement whenever a quantitative analysis is to be carried out, following identification. The combined use of PDA and MS data allowed to distinguish among thirty-three carotenoids contained in the sample (Table 4).

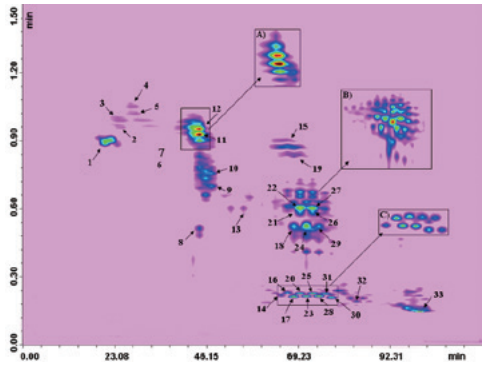

Figure 10. Contour plot of the NP-LC×RP-UHPLC analysis of free carotenoids and carotenoid esters present in a red chili pepper extract with a modulation time of 1.50 min (PDA chromatogram extracted at 450 nm). For experimental conditions see the text. For peak identification see Table 4. The insets show the retention windows corresponding to the di-ol-mono-keto-di-ester (A), the di-ol-mono-keto-mono-ester (B), and the poly-oxygenated-free-xanthophyll (C) classes, separated within 1.00 min 2D gradient and modulation time

NP-LC×UHPRP-LC conditions

Given the possibility to operate the LC×LC system under ultra-high-pressure conditions, another C18 column of the same dimensions could be serially connected, thus reaching a total 6-cm length of fused-core stationary phase in the 2D. In order to keep retention factors constant, the gradient elution program was adapted on the coupled columns by extending the 2D analysis time from 0.75 min (for a single, 30 mm long column) to 1.50 min (for total 60 mm stationary phase), along with the modulation time of the switching valves (cycle time, 1.50 min). The experimental backpressure increased up to roughly 900 bar, at a temperature of

A good correlation was found between the theoretical and the experimentally observed m/z ions obtained using the hybrid IT-TOF analyzer, yielding accuracy values lower than 6 ppm; moreover, it is noteworthy that the complementary information attained allowed to discriminate between compounds showing similar (or nearly identical) UV-absorption properties, arising from the same chromophore groups. An example is represented by the two mono-ol-esters labelled as 2 and 3 in Table 4, namely β-cryptoxanthin-C14:0 and its longer homologue β-cryptoxanthin-C16:0: the absorption spectra of these two molecules in fact overlap, while

the m/z pseudomolecular ions allow to easily distinguish one from the other. On the other hand, mutatoxanthin-C12:0, C16:0 and capsanthin-C14:0,C14:0 (compounds 7 and 12 in Table 4, respectively) having the same molecular formula gave identical [M].- ions; nevertheless different fragment ions (detected in the positive ionization mode) and totally different UV maxima render discrimination of the di-ol-mono-epoxide-di-ester and the di-ol-mono-keto-di-ester straightforward.

Further improvement of the LC×LC system was attained by reducing the modulation time by a factor of 1/3, i.e. from 1.50 to 1.00 min with the stepwise gradient modified, accordingly. Better fractionation of the 1D eluate improved the chromatographic separation. For a quantitative estimation of the increase in resolution between these classes, the peak separation index (P.S.I.) was compared, as obtained between critical pairs by the two NP-LC×RP-UHPLC systems, viz. set-up #2 and set-up #3. An example is illustrated by compounds listed as 11 and 12 in Table 4, numbered correspondingly in the 2D plot, identified as capsanthin-C12:0,C14:0 diester and its longer analogue, namely capsanthin-C14:0, C14:0. Their very similar chemical structures, differing in only two carbon units at acyl chain length, are responsible in very similar retention behavior (and degree of co-elution); nevertheless, the separation between these compounds increased from 0.61 in the NP-LC×RP-UHPLC analysis at 1.50 min modulation time, to 0.71 in the corresponding analysis at 1.00 min.

A larger degree of chromatographic separation is, undoubtedly, beneficial prior to PDA or MS detection, for identification of the separated compounds, and becomes mandatory if quantitation is to be carried out, at the desired level of accuracy. Quantitative evaluation of all the sample components was not carried out, at this level, due to the scarce availability of pure reference material; however, a rough estimation of the different chemical class amounts would be possible, through software integration of the corresponding regions in the plot.

From the calculated relative percentage areas attained, the most abundant carotenoid compounds in the sample belong to the di-ol-mono-keto-mono-ester class, accounting for nearly 36% of the whole carotenoid content, followed in order by the di-ol-mono-keto-di-esters (21.%), the poly-oxygenated-free-xanthophylls (16%), and the di-ol-mono-epoxide-mono-esters (12%). The remaining classes were in the 1-6% amount, with the exception of di-ol-mono-epoxide-di-esters which were only present at trace level.

Table 4. NP-LC×RP-UHPLC/PDA and LCMS-IT-TOF (APCI) carotenoid fingerprint in a red chili pepper extract.

N°	Compound	[M-H]- observed	Error (ppm)	Fragment ions*	Class
1	β-carotene	536.4392	1.86	-	Hydrocarbons
2	β-cryptoxanthin-C14:0	762.6319	0.52	535	Mono-ol-esters
3	β-cryptoxanthin-C16:0	790.6659	3.92	535	
4	Zeaxanthin-C14:0,C14:0	988.8227	-2.12	761,533	Di-ol-di-esters
5	Zeaxanthin-C14:0,C16:0	1016.855	-0.88	798,761,533	
6	Mutatoxanthin-C12:0,C14:0	976.784	-4.5	777,749,549	Di-ol-mono-epoxide-di-esters, trace amounts
7	Mutatoxanthin-C12:0,C16:0	1004.815	-5.07	805,749,549	
8	β-cryptoxanthin	552.4312	-3.44	535	Free mono-ols
9	Antheraxanthin-C12:0	766.594	5.21	749,567	Di-ol-mono-epoxide-mono-esters
10	Antheraxanthin-C14:0	794.6216	0.38	777,567	
11	Capsanthin-C12:0,C14:0	976.7843	-4.19	777,749,549	Di-ol-mono-keto-di-esters
12	Capsanthin-C14:0,C14:0	1004.815	-4.48	777,549	
13	Mutatoxanthin-C14:0	794.6228	1.88	777,567	Di-ol-mono-epoxide-mono-esters
14	(9Z) Lutein	568.4283	0.53	551	Poly-oxygenated-free-xanthophylls
15	Capsorubin-C14:0,C14:0	1020.814	-0.19	793,565	Di-ol-di-keto-di-esters
16	Isolutein	568.4262	-3.16	551	Poly-oxygenated-free-xanthophylls
17	Antheraxanthin	584.4244	2.56	567	
18	n.i.	-	-	567	Di-ol-mono-keto-mono-esters
19	Capsorubin-C12:0,C14:0	992.786	2.72	793,765,565	Di-ol-di-keto-di-esters
20	Violaxanthin-type	-	-	601,583	Poly-oxygenated-free-xanthophylls
21	Capsanthin- C12:0	766.5928	3.65	567,549	Di-ol-mono-keto-mono-esters
22	Capsanthin-C14:0	794.6246	4.16	777,567	
23	Antheraxanthin-type	-	-	567	Poly-oxygenated-free-xanthophylls
24	Capsanthin-monoester	-	-	567,549	Di-ol-mono-keto-mono-esters
25	Antheraxanthin-type	-	-	567	Poly-oxygenated-free-xanthophylls
26	Capsanthin-monoester	-	-	567,549	Di-ol-mono-keto-mono-esters
27	Capsanthin-monoester	-	-	567,549	
28	Antheraxanthin-type	-	-	567	Poly-oxygenated-free-xanthophylls
29	Capsanthin-monoester	-	-	567,549	Di-ol-mono-keto-mono-esters
30	Zeaxanthin	568.4261	-3.34	569,551,476	Poly-oxygenated-free-xantN° hophylls
31	Zeaxanthin-type	-	-	569,551,476	
32	Mutatoxanthin	584.4234	0.85	585,567,549	
33	Capsanthin	584.4252	3.93	585,567	

Evaluation of the system performances

Main differences of the three instrumental set-ups developed for the sample analysis, are highlighted in Table 5, which also reports the relative performance of the gradient separations, in terms of peak capacity, nC. The latter, was calculated using the method defined by Neue [15]. A total of eight chromatographic peaks were selected for the calculation, arising from representative components eluting over the spanning time scale.

1D column and analysis conditions were kept constant in all the three instrumental set-ups developed, affording a calculated nC of 45 for a 110 min linear gradient separation. In the NP-LC×RP-LC analysis (set-up #1), a 30 mm long column was used for 2D separation, operated under stepwise 0.75 min gradient, including 0.04 min for column re-equilibration. A peak capacity value of 22 was estimated, for this separation. The overall peak capacity of the NP-LC×RP-LC separation, obtained with a modulation time of 0.75 min, was calculated as 990 (theoretical 2DnC,), being multiplicative of the individual values obtained for the two dimensions (nC1 × nC2). When switching to NP-LC×RP-UHPLC configuration (set-up #2), the 2D stationary phase was elongated, by serially coupling two identical columns for a total length of 60 mm, with the aim of increasing the separation power. In order to keep retention factors constant, the mobile phase gradient was modified, accordingly, to twice the duration (from 0.75 to 1.50 min). As predictable, the 2D peak capacity increased by a 40% factor, to a value of 31, as a result of the proportional increase in efficiency (N increase by a factor of 2) and resolution (R_S increase by a factor of $\sqrt{2}$). As a consequence, the theoretical peak capacity was substantially increased, to a calculated nC1×nC2 value of 1395, when coupling the two dimensions in the comprehensive set-up #2, and adapting the modulation time to the new 2D gradient, i.e. 1.50 min.

Further development of the LC×LC system consisted in reducing the 2D gradient time to 1.00 min, while keeping the same column length, and decrease the sampling interval to the same period (set-up #3). The performance of this latter set-up is decreased, apparently, with respect to set-up #2, to a theoretical value of 1125, due to a proportional decrease of 2D peak capacity (25). However, these values are merely theoretical, and highly inflated, without taking into account effects of the first dimension under-sampling (fractions transferred), or the selectivity correlation (orthogonality), or the retention window in both dimensions, which does not cover the whole gradient duration. For the quantitative estimation of the under-sampling effect, a very recent approach developed by Carr' s research group was employed [16], which takes into account the second dimension cycle time, which in our experiment settings is equal to the first dimension sampling time (and equal to the 2D gradient time, plus the 2D re-equilibration time), and the average first dimension peak width. By applying such a calculation, the under-sampling effect was estimated as 1.15, 2.54, and 1.44, for set-up #1, set-up #2, and set-up #3, respectively.

The number of fractions effectively transferred from the first dimension could be calculated (by simply dividing the 1D gradient time by the modulation time) as equal to 147, 73, and 110, for set-up #1, set-up #2, and set-up #3, respectively.

Last, quantitative evaluation of orthogonality between the two dimensions was made, for the three instrumental set-ups developed, using an equation proposed by Liu et al. [17], which is based on solute retention parameters and, therefore, it is more accurate in describing resolving power with respect to those calculated by the multiplicative rule. Despite the coupling of independent separation modes in the two dimensions (NP-LC×RP-LC), a certain degree of retention correlation was observed in all the 2D systems developed, not truly orthogonal. In order to calculate the under-sampling, and the orthogonality effects on the system performance in a cumulative way, the "practical" peak capacities, as reported in Table 5, were calculated. Practical peak capacities values in Table 5 show that, when switching from NP-LC×RP-LC (set-up #1) to NP-LC×RP-UHPLC at 1.50 min modulation time (set-up #2), the performance of the system is greatly affected from undersampling of the first dimension peaks, since a longer gradient and an equal modulation time were employed in 2D, on the coupled columns.

On the other hand, LC×RP-UHPLC at 1.00 min modulation time (set-up #3) yielded the best results in terms of performance; in fact, whilst a reduced 2D peak capacity was obtained, with respect to set-up #2, yet the under-sampling effect (estimated as 1.44) affected the total nC value of the LC×LC system to a lesser extent.

Table 5. Columns and experimental settings of the three instrumental set-ups developed for the sample analysis, as well as the relative performances, in terms of peak capacity, nC.

		SET-UP #1	SET-UP #2	SET-UP #3
^1D	Column	250 x 1.0 mm, 5.0 µm	250 x 1.0 mm, 5.0 µm	250 x 1.0 mm, 5.0 µm
	Gradient	110 min, linear	110 min, linear	110 min, linear
	n_c	45	45	45
^2D	Column	30 x 4.6 mm, 2.7 µm	2x 30 x 4.6 mm, 2.7 µm	2x 30 x 4.6 mm, 2.7 µm
	Gradient*	0.75 min, stepwise	1.50 min, stepwise	1.00 min, stepwise
	Mod. time	0.75 min	1.50 min	1.00 min
	n_c	22	31	25
	Theoretical	990	1395	1125
^2Dn_c	Corrected	858	558	775
	Effective	727	377	984

4. CONCLUSIONS

In this contribution, several analytical approaches have been tested on different *Capsicum* species to investigate carotenoid composition. The on-line SFE-SFC system has proven to be a much faster method compared to off-line approaches, drastically reduces the extraction time (compared to the traditional solid/liquid extraction, which required about a couple of hours), reduces the analysis run time, reduces the risk of sample contamination, improves run-to-run precision, and enables the setting of batch-type applications. In fact, considering both extraction process and chromatographic run, the developed method run-time is 18 min. Regarding the RP-HPLC methodology reported in this work, it has been demonstrated to be a valid and instrumentally quite simple way to further improve resolution and efficiency in LC; in addition, apart from a very early report of Philip et al. [18] on the carotenoids esters in sweet red bell peppers carried out by gas chromatographic analysis of the transesterified fatty acids obtained after saponification and which reported some generic tentative identifications, the work here reported shows the first direct study on the native carotenoids composition in sweet bell peppers using a liquid chromatographic methodology. In fact, previous works on the carotenoid composition of sweet bell peppers [19-23] were carried out after a saponification step. Finally, the NP-LC×RP-LC system developed was successfully applied to analysis of the intact carotenoid composition of red chili peppers. UHPLC conditions were subsequently exploited in the 2D, by doubling the length of stationary phase.

Modulation times of 1.50 and 1.00 min were employed, corresponding to the 2D analysis time. From a performance comparison of three different set-ups, in terms of peak capacity values (nc), the NP-LC×RP-UHPLC with a 1.00 min modulation time (and gradient) turned out to be the most effective, affording a peak capacity value as high as 984. Despite the doubling of the stationary phase length, with respect to the "conventional" NP-LC×RP-LC set-up, the NP-LC×RP-UHPLC method with a 1.50 min modulation time (and gradient), greatly suffered the reduced number of fractions, transferred from the first dimension. Up to thirty-three components belonging to ten different chemical classes were successfully identified in the sample tested, by the complementary information afforded by the two detection techniques.

Much space is, undoubtedly, left for optimization of the system, both in terms of separation/identification power, and reliable quantitation of the separated components.

5. REFERENCES

[1] D. Giuffrida, P. Dugo, G. Torre, C. Bignardi, A. Cavazza, C. Corradini, G. Dugo. Food Chemistry 140 (2013) 794–802.

[2] D.A. Kopsell, D.E. Kopsell (2010). Carotenoids in vegetables: Biosynthesis, Occurrence, Impacts on Human health, and Potential for Manipulation. In Bioactive Food in Promoting Health, R.R. Watson, V.R. Preedy eds., Academic Press, London, 645.

[3] Beutner S, Bloedorn B, Frixel S, Hernandez Blanco I, Hoffman T, Martin H D, Mayer B, Noack P, Ruck C, Schmidt M, Schulke I, Sell S, Ernst H, Haremza S, Seybold G, Sies H, Stahl W, Walsh R. (2001) Quantitative assessment of antioxidant properties of natural colorants and phytochemicals: carotenoids, flavonoids, phenols and indigoids. The role of b-carotene in antioxidant functions. Journal of Science Food & Agriculture 81, 559-568.

[4] Minguez-Mosquera MI, Hornero-Mendez D. (1994) Changes in carotenoid esterification during the fruit ripening of Capsicum annuum Cv. Bola. Journal of Agricultural and Food Chemistry, 42, 640-644.

[5] Hornero-Mendez D, Minguez-Mosquera MI. (2000) Xanthophyll esterification accompanying carotenoid overaccumulation in chromoplast of Capsicum annuum ripening fruits is a costitutive process and useful for ripeness index. Journal of Agricultural and Food Chemistry, 48, 1617-1622.

[6] Schweiggert U, Kammerer DR, Carle R, Schieber A. (2005) Characterization of carotenoids and carotenoid esters in red pepper pods (Capsicum annuum L.) by high-performance liquid chromatography/atmospheric pressure chemical ionization mass spectrometry. Rapid Communications in Mass Spectrometry, 19, 2617-2628.

[7] P. Dugo, M. Herrero, T. Kumm, D. Giuffrida, G. Dugo, L. Mondello, J. Chromatogr. A 1189 (2008) 196.

[8] P. Dugo, M. Herrero, D. Giuffrida, T. Kumm, G. Dugo, L. Mondello, J. Agric. Food Chem. 56 (2008) 3478.

[9] P. Dugo, V. Skerikova, T. Kumm, A. Trozzi, P. Jandera, L. Mondello, Anal. Chem. 78 (2006) 7743.

[10] P. Dugo, D. Giuffrida, M. Herrero, P. Donato, L. Mondello, J. Sep. Sci. 32 (2009) 973.

[11] P. Donato, P. Dugo, F. Cacciola, G. Dugo, L. Mondello, J. Sep. Sci. 32 (2009) 1129.

[12] P. Dugo, F. Cacciola, M. Herrero, P. Donato, L. Mondello, J. Sep. Sci. 31 (2008) 3297.

[13] P. Dugo, F. Cacciola, P. Donato, D. Airado-Rodriguez, M. Herrero, L. Mondello, J. Chromatogr. A 1216 (2009) 7483.

[14] P. Dugo, F. Cacciola, P. Donato, R. Assis Jacques, E.B. Caramao, L. Mondello, J. Chromatogr. A 1216 (2009) 7213.

[15] U. W. Neue, J. Chromatogr. A 1079 (2005) 153.

[16] H.Gu, Y. Huang, P. W. Carr, J. Chromatogr. A 1218 (2011) 64.

[17] Z. Liu, D. G. Patterson, M. L. Lee, Anal. Chem. 67 (1995) 3840.

[18] Gregory GK, Chen TS, Philip T. (1987). Quantitative analysis of carotenoids and carotenoid esters in fruits by HPLC: red bell peppers. Journal of Food Science, 52, 1071-1073.

[19] Sun T, Xu Z, Wu CT, Janes M, Prinyawtwatkul W, No HK. (2007). Antioxidant activities of different colored sweet bell peppers (Capsicum annuum L.). Journal of Food Science, 72, S98-S102.

[20] de Azevedo-Meleiro CH, Rodriguez-Amaya DB. (2009). Qualitative and quantitative differences in the carotenoid composition of yellow and red peppers determined by HPLC-DAD-MS. Journal of Separation Science, 32, 3652-3658.

[21] Matsufuji H, Ishikawa K, Nunomura O, Chino M, Takeda M. (2007). Anti-oxidant content of different coloured sweet peppers, white, green, orange and red (Capsicum annuum L.). International Journal of Food Science and Technology, 42, 1482-1488.

[22] Guil-Guerrero JL, Martinez-Guirado C, Rebelloso-Fuentes M, Carrique-Perez A. (2006). Nutrient composition and antioxidant activity of 10 pepper (Capsicum annuum) varieties. European Food Research and Technology, 224, 1-9.

[23] Marin A, Ferreres F, Tomas-Barberan FA, Gil MI. (2004). Characterization and quantification of antioxidant constituents of sweet pepper (Capsicum annuum L.). Journal of Agricultural and Food Chemistry, 52, 3861-3869.

First Edition: October, 2023

SHIMADZU

Shimadzu Corporation

www.shimadzu.com/an/

3655-08309-PDFIT